Carbohydrate Polymers 330 (2024) 121821

Contents lists available at ScienceDirect

Carbohydrate Polymers

journal homepage: www.elsevier.com/locate/carbpol

Biomimetic zwitterionic copolymerized chitosan as an articular lubricant

Junjie Deng [a,b,c], Rufang Wei [a,b,c], Haofeng Qiu [b,c,f], Xiang Wu [g], Yanyu Yang [a,b,c], Zhimao Huang [b,c], Jiru Miao [b,c], Ashuang Liu [a,b,c], Haiyang Chai [a,b,c], Xiao Cen [d,e,*], Rong Wang [a,b,c,**]

[a] Cixi Biomedical Research Institute, Wenzhou Medical University, Zhejiang 315300, PR China
[b] Zhejiang International Scientific and Technological Cooperative Base of Biomedical Materials and Technology, Institute of Biomedical Engineering, Ningbo Institute of Materials Technology and Engineering, Chinese Academy of Sciences, Ningbo 315201, PR China
[c] Ningbo Cixi Institute of Biomedical Engineering, Ningbo 315300, PR China
[d] State Key Laboratory of Oral Diseases & National Clinical Research Center for Oral Diseases, Sichuan University, Chengdu, 610041, Sichuan, PR China
[e] Department of Temporomandibular Joint, West China Hospital of Stomatology, Sichuan University, No. 14, 3rd Section, South Renmin Road, Chengdu, 610041, Sichuan, PR China
[f] School of Materials Science and Engineering, Nanjing University of Science & Technology, Nanjing 210094, PR China
[g] Ningbo Medical Center Li Huili Hospital; Health Science Center, Ningbo University, Ningbo 315000, PR China

ARTICLE INFO

Keywords:
Osteoarthritis
Cartilage
Chitosan
Zwitterionic copolymer
Adsorption lubrication

ABSTRACT

Restoration of the lubrication functions of articular cartilage is an effective treatment to alleviate the progression of osteoarthritis (OA). Herein, we fabricated chitosan-*block*-poly(sulfobetaine methacrylate) (CS-b-pSBMA) copolymer *via* a free radical polymerization of sulfobetaine methacrylate onto activated chitosan segment, structurally mimicking the lubricating biomolecules on cartilage. The successful copolymerization of CS-b-pSBMA was verified by Fourier transform infrared spectroscopy, X-ray photoelectron spectroscopy, and ^{1}H nuclear magnetic resonance. Friction test confirmed that the CS-b-pSBMA copolymer could achieve an excellent lubrication effect on artificial joint materials such as Ti6Al4V alloy with a coefficient of friction as low as 0.008, and on OA-simulated cartilage, better than the conventional lubricant hyaluronic acid, and the adsorption effect of lubricant on cartilage surface was proved by a fluorescence labeling experiment. In addition, CS-b-pSBMA lubricant possessed an outstanding stability, which can withstand enzymatic degradation and even a long-term storage up to 4 weeks. *In vitro* studies showed that CS-b-pSBMA lubricant had a favorable antibacterial activity and good biocompatibility. *In vivo* studies confirmed that the CS-b-pSBMA lubricant was stable and could alleviate the degradation process of cartilage in OA mice. This biomimetic lubricant is a promising articular joint lubricant for the treatment of OA and cartilage restoration.

1. Introduction

Osteoarthritis (OA) is the most common degenerative joint disease, characterized by the decline of lubrication of articular cartilage (Yuan et al., 2023). Without timely interventions to restore the lubrication of articular cartilage, the increased friction will aggravate the condition and eventually lead to disability (Pap & Korb-Pap, 2015). Therefore, restoring the lubricating properties of articular cartilage is critical in the treatment of OA (Lin & Klein, 2021). Efforts to emulate the super-lubricating property of the articular cartilage matrix have explored the use of lubricants like hyaluronic acid (HA) derivatives. However, challenges persist due to the rapid clearance of HA (Xie et al., 2021). Although lubricants with a polyelectrolyte brush architecture and drug-releasing properties have been recently reported for OA treatment (Chen et al., 2020; Yan et al., 2019; Zhang et al., 2023), issues like rapid initial release and quick drug clearance remain largely unresolved (Ahamad et al., 2020; Kar et al., 2022). Therefore, it is of great significance to develop a straightforward, effective, safe, and long-lasting biomimetic lubricant for the treatment of OA (Yuan et al., 2023).

Several strategies have been used to achieve excellent biomimetic

* Correspondence to: X. Cen, State Key Laboratory of Oral Diseases & National Clinical Research Center for Oral Diseases, Sichuan University, Chengdu, 610041, Sichuan, PR China.
** Correspondence to: R. Wang, Cixi Biomedical Research Institute, Wenzhou Medical University, Zhejiang 315300, PR China.
E-mail addresses: cenx@scu.edu.cn (X. Cen), rong.wang@nimte.ac.cn (R. Wang).

https://doi.org/10.1016/j.carbpol.2024.121821
Received 26 October 2023; Received in revised form 22 December 2023; Accepted 11 January 2024
Available online 15 January 2024

lubrication (Lin & Klein, 2021). One is to construct a coating on the contact surface with the ability to recruit lubricin from the synovial fluid *via* non-covalent interactions, while the lubrication effect of the recruited lubricin alone is limited (Jahn, Seror, & Klein, 2016; Wan, Ren, Kaper, & Sharma, 2020; Wan, Zhao, Lin, Kaper, & Sharma, 2020). Another strategy is covalent grafting of lubrication polymer onto the substrate to form a direct lubricating layer (Liu et al., 2022; Qin, Sun, Hafezi, & Zhang, 2019). However, the irreversibility of covalent bonding and the constant shear force from joint movement could lead to bonding failure and subsequent loss of lubrication (Yue et al., 2022). Although the lubricating layers constructed by physical adsorption of catechol-based polymers are usually reversible, they are susceptible to oxidation, leading to decreased adhesion and lubrication efficiency (Li, Yan, Zhang, Tian, & Zeng, 2015; Park et al., 2021; Shin et al., 2020).

It is reported that the pH of the joint cavity affected by OA tends to be acidic, reaching as low as 6.0 (Jin et al., 2020), which contributes to the protonation of the amino groups of chitosan (CS) and its derivatives. Subsequently, it facilitates a reversible electrostatic interaction between the electronegative cartilage and the electropositive CS polymers, offering effective resistance against repeated shear stress and achieving a sustained lubrication effect (Hamedi, Moradi, Hudson, Tonelli, & King, 2022; Vandeweerd et al., 2021). In addition, CS exhibits excellent biocompatibility and antibacterial properties, as well as a significantly long biodegradability period (Alfaifi, Alkabli, & Elshaarawy, 2020; Goto, Masuda, & Aiba, 2015; Kamal et al., 2021; Nasr et al., 2022). When appropriately designed and functionalized, and considering its economic advantages, CS stands as an ideal candidate for the fabrication of HA-like macromolecules as a biomimetic lubricant (Wang, Xue, & Mao, 2020; Yang et al., 2023; Yang et al., 2023).

The common hydrophilic polymer polyethylene glycol (PEG) and its derivatives are widely used as antifouling lubricating materials, but their long-term application *in vivo* is limited by their biodegradability and immunogenicity (Li et al., 2018; Yang et al., 2020). Poly(sulfobetaine methacrylate) (pSBMA), by contrast, is a zwitterionic polymer that exhibits robust water retention through ionic solvation and displays superior lubrication property (Zhu et al., 2021). Due to its structural stability and biocompatibility, pSBMA has obvious advantages as a lubricating material for OA treatment (Li et al., 2022). For example, pSBMA-based block polymers were used to modify nanoparticles to enhance interface lubrication and reduce inflammation in OA (Chou, Chang, & Wen, 2015; Zhang et al., 2023).

In a previous study, we prepared a block copolymer of CS and SBMA (denoted as CS-b-pSBMA) *via* polymerization of SBMA chain onto CS segment for developing antibacterial and antifouling coatings (Wang, Neoh, & Kang, 2015). Considering the distinctive cationic properties of CS and the excellent lubricating properties of pSBMA, this study aims to explore the potential application of CS-b-pSBMA copolymer in lubrication and cartilage repair. The lubrication performance of the CS-b-pSBMA copolymer on various artificial joint materials and degenerated porcine articular cartilage was evaluated. The resistance and stability of the lubricant against enzymatic degradation and prolonged aging were studied. The possible mechanism of the lubricating effect of the copolymer was explored. In addition, the *in vitro* antibacterial properties and cytotoxicity, as well as the *in vivo* performance of the lubricant after injection into OA mice were investigated.

2. Materials and methods

2.1. Materials

Chitosan (CS, molecular weight: 1,200–2,500 kDa, deacetylation degree: ≥ 95 %, viscosity: 100–200 mPa•s (data obtained from the supplier)), sulfobetaine methacrylate (SBMA), and ammonium persulfate (APS) were purchased from Aladdin Chemistry (Shanghai, China). Hyaluronic acid (HA, molecular weight: 1,800 kDa (data obtained from the supplier)) was purchased from Bloomage Biotechnology (Jinan, China). Ti6Al4V alloy plate (TC4, 43 mm × 30 mm × 2 mm), purchased from Baoji Titanium Industry (Baoji, China), was polished with 240 mesh, 320 mesh, 400 mesh, 600 mesh, 800 mesh, 1,000 mesh, 1,200 mesh, and 1,500 mesh abrasive paper 5–10 min for each step, and finally polished with 15,000 mesh abrasive pastes. Ultra-high molecular weight polyethylene (UHMWPE) was gained from Wear-Resistant Materials Co., LTD (Shandong, China). Aluminum oxide plate (Al_2O_3) (43 mm × 30 mm × 2 mm) was obtained from Baile New Materials Co., LTD (Guangzhou, China). SYL-GARD™ 184 Silicone Elastomer Kit was obtained from Dow Chemical (Michigan, United States), and used to prepare polydimethylsiloxane (PDMS) hemispheres (diameter of 6 mm) molded with a U-shaped bottom 96-well plate. *Staphylococcus aureus* (*S. aureus*) 5622 was a gift from the First Affiliated Hospital of Ningbo University. *Escherichia coli* (*E. coli*) ATCC 25922 was obtained from American Type Culture Collection.

2.2. Polymer synthesis

CS-b-pSBMA copolymer was synthesized following the previous work (Wang, Neoh, & Kang, 2015). Briefly, CS (0.5 g) was completely dissolved in 30 mL of 1 % acetic acid solution at 60 °C. The solution was degassed using nitrogen flow bubbling for 30 min, and followed by addition of 100 mg of APS. After 30 min for generation of free radicals by decomposition of APS and cleaving of CS chain, 20 mL of SBMA aqueous solution (containing 4.57 g of SBMA monomers) was added dropwise to the solution at a constant rate of ≈0.67 mL/min over 30 min. The reaction temperature was maintained at 60 °C, and nitrogen bubbling continued for 6 h. Finally, the product was collected and dialyzed in deionized water using a cellulose dialysis bag (molecular weight cutoff: 8000–14,000 Da) for 72 h, and freeze-dried. It should be admitted that pSBMA homopolymer could be produced in the reaction, and those with molecular weight higher than 8000–14,000 Da inevitably remained in the product. pSBMA homopolymer was synthesized under the same procedure using SBMA monomer (20 mL solution at a concentration of 0.23 g/mL) but without CS.

2.3. Polymer characterization

The polymers were characterized using Fourier transform infrared (FT-IR) spectroscopy (Nicolet-iS50, ThermoFisher), X-ray photoelectron spectroscopy (XPS, Axis Ultra DLD, Shimadzu), and ^{1}H Nuclear magnetic resonance (^{1}H NMR, AVANCE NEO 400 MHz, Bruker, with deuterate water as the solvent). CS segment after APS treatment (denoted as CS-) was determined following a viscometrical method. The content of carbon, nitrogen, and sulfur in CS-b-pSBMA copolymer was analyzed by an elemental analyzer (FlashSmart™ Thermo Fisher). The zeta potential of the polymer solutions and the hydrated particle size of copolymer were measured *via* dynamic light scattering (DLS, Zetasizer Advance ZSU3305, Malvern Instruments). The viscosity of copolymer in water was determined using rotating rheometer (Discovery HR-2, TA Instruments). The experimental details are given in the Supporting Information.

2.4. Tribological test

A PDMS hemisphere (diameter of 6 mm) and a polished plate (Ti6Al4V alloy, glass, Al_2O_3 or UHMWPE with size of 43 mm × 30 mm × 2 mm) were used to form the friction pair and fixed in a UMT Bruker TriboLab pin-on-plate tribometer (Bruker, Germany). The contacting interface of the friction pair was ensured to be immersed in the lubricant solution (10 mg/mL HA in water, 0.01–100 mg/mL of CS-b-pSBMA lubricant prepared by water, physiological saline solution (0.9 % NaCl), phosphate-buffered saline buffer (PBS, 10 mM, pH = 7.2–7.4) or bovine serum albumin (BSA) solution (0.1 mg/mL)). Generally, without special instructions, the PDMS hemisphere traveled on the base plate in the presence of lubricant solution under a constant loading force of 10 N,

corresponding a pressure of 1.08 MPa calculated by the Hertz contact theory (details in Supporting Information), which is approximated the mean physiological pressure of human articular cartilage (*i.e.*, 10 atm ≈ 1 MPa) (Lin & Klein, 2021; Rong et al., 2020). The single travelling distance was 10 mm, and the running time was 900 s or 3600 s, while the travelling speed was 10 mm/s (maximum value achieved by the device), which is within the range of the sliding speed of human synovial joints (*i.e.*, 0–300 mm/s) (Macirowski, Tepic, & Mann, 1994). The coefficient of friction (COF) was defined as the absolute value of the frictional force divided by the load force, and calculated by the data processing software of the UMT TriboLab (Data Viewer, Version 2.22.115. Build 2).

For measurement of the lubricating effect of polymer solution on cartilage, a cylindrical bone tissue with the cartilage layer on top (diameter of 4 mm, cartilage thickness: ≈1–2 mm) was obtained by drilling from a fresh pig femoral head (purchased from a local market). The sample was digested in 0.25 % trypsin for 1 h to obtain an OA-like cartilage. It was then fixed using a customized setup and loaded in the tribometer. The COF of cartilage on polished Ti6Al4V alloy plate in the presence of lubricant solution was measured as described above. The cartilage after friction was fixed with 4 vol% paraformaldehyde and then dehydrated with gradient ethanol. After evaporation of ethanol, the surface was observed using a scanning electron microscope (SEM, S4800. Hitachi).

2.5. Adsorption effect of copolymer on cartilage surface

Ten mL of 10 mg/mL CS-b-pSBMA solution was mixed with 5 mL of fluorescein isothiocyanate (FITC, Macklin, China) methanol solution (2 mg/mL), and reacted in dark for 6 h. It was then washed with methanol, and centrifuged to separate the supernatant without fluorescence detection to obtain FITC-labeled CS-b-pSBMA copolymer, which was then freeze-dried. Cartilage sample (same as that in the lubrication test) was immersed in 200 μL of the FITC-labeled CS-b-pSBMA solution (1 mg/mL, pH of 6 or 13 adjusted by acetic acid or sodium hydroxide solution) for 1 min, and then washed with ultrapure water for 3 times, and dried with filter paper. The cartilage sample was cut into longitudinal slices and attached to a glass slide. Fluorescence distribution on the edge of the cartilage was recorded by confocal laser scanning microscopy (TCS SP8, Leica), and quantitatively analyzed using ImageJ software (Version 1.54d).

2.6. In vitro antibacterial assay

Overnight bacterial cultures of *E. coli* and *S. aureus* were collected by centrifugation and serially diluted with sterilized PBS (10 mM, pH = 7.2–7.4) containing 1 vol% of medium (Lysogeny broth for *E. coli* and Tryptic Soy Broth for *S. aureus*) to a bacterial suspension concentration of 10^6 cells/mL. After that, 1 mL of the prepared bacterial suspension was added to 9 mL of PBS solution (containing 1 vol% of the respective medium) of CS-b-pSBMA at a concentration of 1 mg/mL to culture for 24 h, while the control group was PBS solution (10 mM, pH = 7.2–7.4, containing 1 vol% of medium) with the same concentration of bacteria. At 0, 1, 6, 12, and 24 h, the viable bacteria in the suspension were counted using the spread plate method after serial dilution.

2.7. In vitro cytotoxicity assay

Chondrocytes that isolated from the knee cartilage of 5-day-old Sprague-Dawley (SD) rats were used to evaluate the potential cytotoxicity of the polymers. The chondrocytes were cultured in Dulbecco's Modified Eagle's Medium (DMEM) supplemented with 10 vol% fetal bovine serum (Gibco, United States) and 1 vol% penicillin-streptomycin (Gibco, United States) and a density of 5000 cells per well (100 μL each well) in a 96-well plate at 37 °C in a humidified 5 vol% CO_2 incubator. After 24 h of growth, DMEM containing different concentrations of CS-b-pSBMA copolymer was used to replace the culture medium. The cells were incubated for 24, 72, and 120 h, and the cell viability was measured using the Cell Counting Kit-8 (CCK-8, Beyotime, China) assay as per the instruction. Complete DMEM medium without copolymer was used as the negative control group, and medium containing 1 vol% Triton-X as the positive control group. Cell viability was expressed as the absorbance value of the experimental group relative to the negative control group.

For microscopy observation, chondrocytes were cultured in a 24-well plate at a density of 20,000 cells per well (1000 μL each well). After 24 h of growth, the culture medium was replaced with DMEM containing different concentrations of CS-b-pSBMA copolymer. The cells were further incubated for 72 h, stained by Calcein/PI Cell Viability/Cytotoxicity Assay Kit (Beyotime, China), and observed using a fluorescent microscope (DMi8, Leica).

2.8. Biodegradation of lubricant

To evaluate the stability of the lubricant against enzymic degradation, CS-b-pSBMA solution (1 mg/mL) or HA solution (10 mg/mL) was treated with lysozyme (LZ, 0.1 mg/mL) or hyaluronidase (HAase, 100 U/mL) at 37 °C for 48 h, and its lubricating performance was measured as described above. In addition, CS-b-pSBMA solution (1 mg/mL) was incubated in a 37 °C shaker for up to 28 days, and the lubricating performance of the copolymer solution was tested on the pre-determined days.

As for assessment of the degradation rate *in vivo*, 200 μL fluorescently labeled lubricant (FITC-CS-b-pSBMA) was subcutaneously injected into mouse (C57 BL/6 N mouse, female, 16–18 g, 6–8 weeks). All of the animal experiments were performed in compliance with the principles of the National Research Council's Guide for the Care and Use of Laboratory Animals, and the Laboratory animal - Guideline for ethical review of animal welfare (GB/T 35892–2018), and approved by the Institutional Animal Ethical Committee of West China Hospital of Stomatology, Sichuan University (approval number: WCHSIRB-D-2023-163). The fluorescence signals under the skin of the mice were recorded using *In Vivo* Imaging System (IVIS, Lumina XRMS Series III, PerkinElmer) over 28 days.

2.9. Animal study

The therapeutic effect of lubricant on OA was evaluated using a mouse model (C57 BL/6 N mouse, female, 16–18 g, 6–8 weeks). After acclimating for a week, the mice were allocated randomly to the sham, NaCl, HA, and CS-b-pSBMA groups. Ten μL solution containing 0.1 mg of sodium iodoacetate (MIA) was injected into the right hind (RH) knee joint of each mouse on Day 0. After 7 days, the mouse showed significant mechanical hypersensitivity, indicating OA occurred in the animal (Fang et al., 2023). Ten μL of physiological saline solution, HA solution (10 mg/mL), or CS-b-pSBMA physiological saline solution (1 mg/mL) was injected into the OA joint of the mice on Day 7 and Day 21. Finally, all the mice were sacrificed on Day 35, and the RH knee was harvested for micro-computerized tomography scanning (micro-CT, μCT50, SCANCO, Switzerland), or sectionized and stained with hematoxylin and eosin (H&E, Solarbio, China), Toluidine blue (Solarbio, China), and Safranin O-fast green (Solarbio, China) staining for histological analysis. For immunohistochemical staining, rabbit polyclonal anti-SOX9 (HUABIO, China) / matrix metalloproteinase 13 (MMP13, Proteintech, United States) antibodies were used to incubate the sections overnight at 4 °C. After incubating with goat anti-rabbit secondary antibodies for 1 h, the sections were allowed to react with DAB reagents. Appropriate negative controls without primary antibodies were included in immunohistochemistry protocols to confirm specificity. The relative expressions of SOX9 and MMP13 were quantified using ImageJ software (Version 1.54d).

2.10. Statistical analysis

All data were presented as means ± standard deviation ($n \geq 3$). Statistical analyses were performed by paired-samples *t*-test, and differences were considered statistically significance when $p < 0.05$.

3. Results and discussion

3.1. Polymer synthesis and characterizations

For the synthesis of CS-b-pSBMA copolymer (Scheme 1a), the long chains of CS were cleaved by the free radicals from decomposition of persulfate anions and generated shorter polysaccharide segments containing free radicals for subsequent polymerization with SBMA monomers, thereby producing linear block copolymers of CS-b-pSBMA (Ganji & Abdekhodaie, 2008; Wang, Neoh, & Kang, 2015). In general, CS with a high molecular weight and a high deacetylation degree is beneficial for cartilage surface adsorption because of the large number of charged groups on the CS chains (Lee, Lim, Israelachvili, & Hwang, 2013; Lim, Hwang, & Lee, 2021; Lim, Lee, Israelachvili, Jho, & Hwang, 2015). Therefore, CS with high molecular weight and high deacetylation degree was used for activation in this study to ensure the CS fragment after APS cleavage (CS-) to serve as macromolecular radicals. The molecular weight of CS- is about 38 kDa (details in Supporting Information) with zeta potential of +10.4 mV in aqueous solutions (Fig. S1a), which still possess the capability of adsorption onto cartilage (Bajpayee & Grodzinsky, 2017).

The successful synthesis of CS-b-pSBMA block copolymer was first verified by observation of the solubility of the polymers in water (Fig. 1a). At the same concentration (1 mg/mL), CS and mixture of CS and pSBMA (containing 1 mg/mL of CS and 1 mg/mL of pSBMA) were insoluble in water, while the CS-b-pSBMA copolymer was fully dissolved in water quickly. This is due to the introduction of sulfobetaine groups in the block copolymer, which increases its water solubility. The chemical composition of CS-b-pSBMA copolymer, pure CS and pSBMA were characterized by FT-IR (Fig. 1b). The spectrum of CS displayed the existence of distinctive absorption peak at 3451 cm^{-1}, which are attributable to the primary hydroxyl (O—H). Weak absorption peaks were observed at 2921 cm^{-1} and 2869 cm^{-1} for asymmetric and symmetric of C—H, while the peaks at 1592 cm^{-1} and 1065 cm^{-1} correspond to the bending of N—H and the C-O-C bridge, respectively (Hamodin, Elgammal, Eid, & Ibrahim, 2023; Ibrahim et al., 2022). Comparing with CS, the spectrum of CS-b-pSBMA shows new absorption peaks at 1724 cm^{-1}, 1475 cm^{-1}, and 1168 cm^{-1} / 600 cm^{-1}, corresponding to the groups of carbonyl ester (O=C-O), quaternary ammonium group (N^+C_4) and sulfonate (SO_3^-) in pSBMA, indicating pSBMA had been successfully introduced into the CS segment (Wang, Neoh, & Kang, 2015). Moreover, the chemical composition of CS-b-pSBMA copolymer was analyzed by XPS. It was found that the N 1 s peak at 399.2 eV, 400.1 eV, and 402.2 eV could be attributed to N—H, and N-H^+ in CS, and N_4^+C in pSBMA, respectively, suggesting the successful copolymerization of pSBMA and CS (Fig. 1c). The chemical information of CS-b-pSBMA copolymer was further determined by ^{1}H NMR (Fig. 1d). The weak peaks at 4.73 ppm, 3.10 ppm and 3.54–4.46 ppm were assigned to the proton signal of the CS backbone of H1, H2, H3-H6 (Ganji & Abdekhodaie, 2008). The resonance signal at 3.19 ppm was attributed to H11 of methyl ($-N^+-CH_3$) in pendant groups of pSBMA chains. The results from FT-IR, XPS, and ^{1}H NMR measurements further confirmed the successful synthesis of CS-b-pSBMA block copolymer.

The contents of carbon, nitrogen, and sulfur in the CS-b-pSBMA copolymer were determined using elemental analyzer (Table S1). The S/N ratio was calculated to be 0.624, and the [SBMA]/[CS] ratio of CS-b-pSBMA copolymer was calculated to be 1.66 (details in Supporting Information). The zeta potential of CS, CS-, and CS-b-pSBMA copolymer was also measured in water at pH 6. It decreased from +29.7 mV of CS to +10.4 mV of CS- (after APS treatment) (Fig. S1a), which may be due to cleavage of the CS polymer chains and incorporation of anionic sulfate ions (Chang, Lin, Wu, & Tsai, 2015). Not surprisingly, the zeta potential of CS-b-pSBMA copolymer was +12.9 mV and the cationic property of CS was well preserved, which will be beneficial to the electrostatic adsorption onto the cartilage interface. Due to the difference in hydrophilicity between CS and pSBMA segments in the CS-b-pSBMA

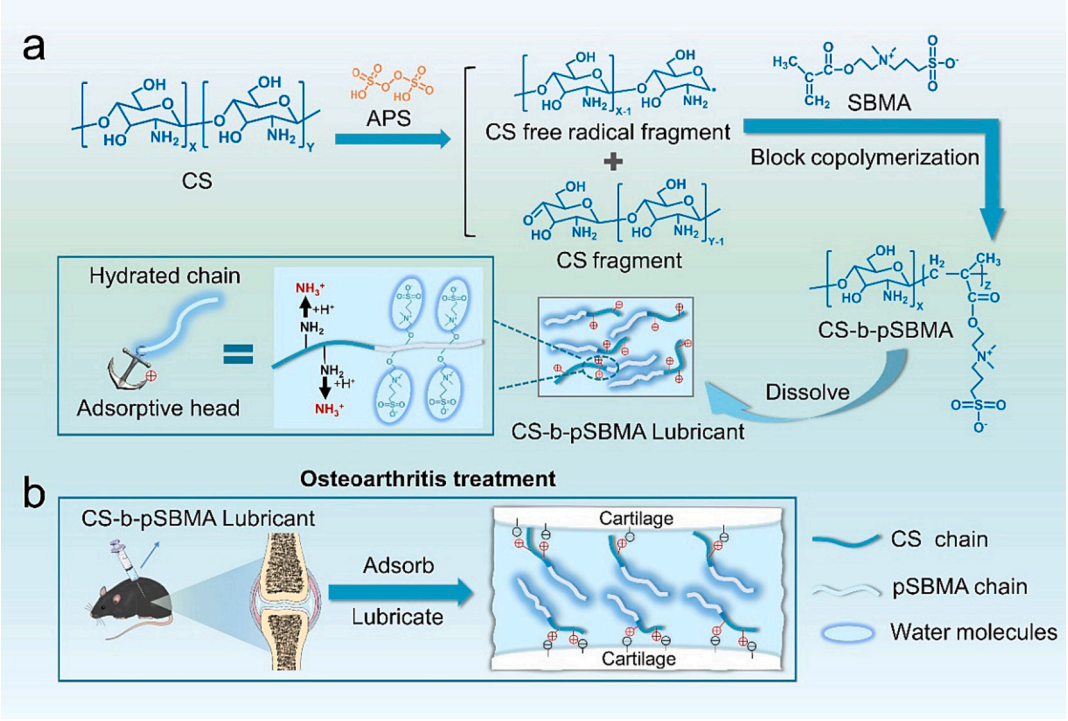

Scheme 1. Schematic illustration of (a) synthesis of CS-b-pSBMA block copolymer, and (b) CS-b-pSBMA lubricant adsorbs onto cartilage surface for lubrication and OA treatment.

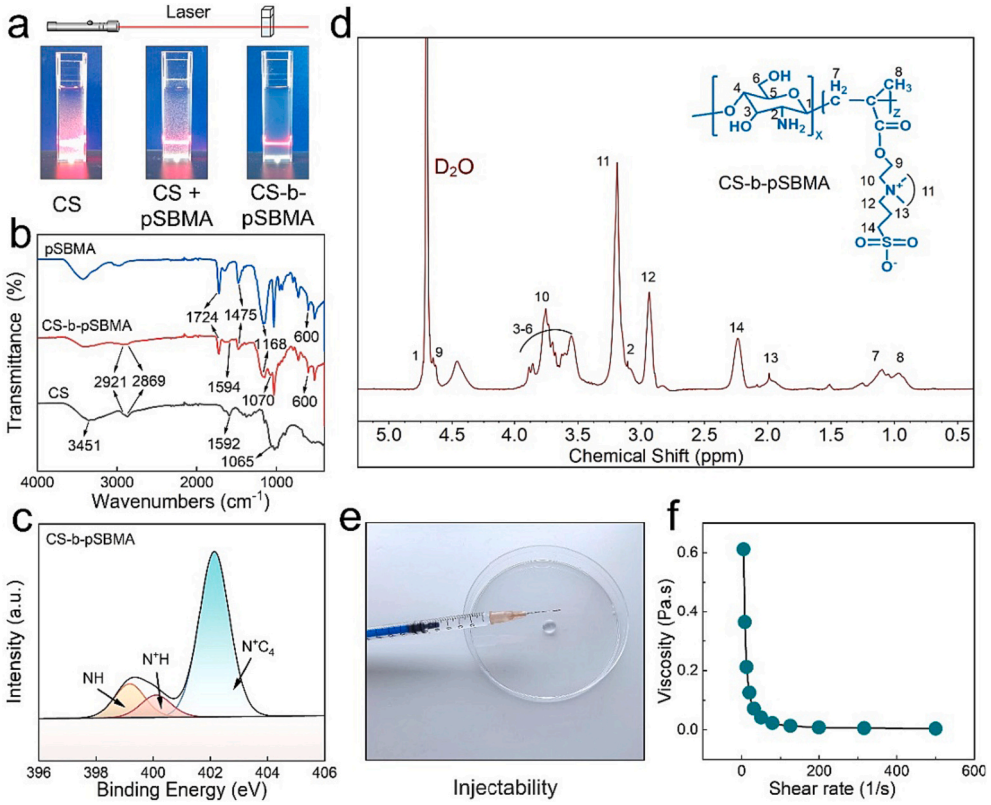

Fig. 1. Characterization of CS-b-pSBMA copolymer. (a) Distribution of CS (1 mg/mL), CS and pSBMA mixture (containing 1 mg/mL of CS and 1 mg/mL of pSBMA), and CS-b-pSBMA copolymer (1 mg/mL) in water. (b) FT-IR spectra of CS, CS-b-pSBMA copolymer, and SBMA monomer. (c) XPS N 1 s core-level spectrum of CS-b-pSBMA. (d) ^{1}H NMR spectrum and molecular structure of CS-b-pSBMA copolymer. (e) Injectable property and (f) viscosity of CS-b-pSBMA copolymer solution (1 mg/mL).

copolymer, it tends to self-assemble in water. The average size of hydrated particles of CS-b-pSBMA was determined to be 487 nm (Fig. S1b). More importantly, the CS-b-pSBMA solution (1 mg/mL) showed remarkable injectability (Fig. 1e), and significant fluidity with the viscosity coefficient close to zero at a shear rate $> 100\ s^{-1}$ (Fig. 1f). The viscosity of CS-b-pSBMA solution under different shear rates decreased obviously from ~0.1 Pa.s at a low shear rate ($1\ s^{-1}$) to ~0.05 Pa.s at a high shear rate ($100\ s^{-1}$), and it recovered rapidly when the shear rate returned, indicating the CS-b-pSBMA solution has an obvious thixotropy (Fig. S2).

3.2. Lubrication performance

The lubricating property of the copolymer was evaluated using a pin-on-plate tribometer. Polished Ti6Al4V alloy and PDMS hemisphere was chosen as the substrate and the friction head to form the friction pair, which was immersed in the lubricant solution (Yue et al., 2022). The COF value was measured by the tribometer in the form of linear reciprocating motion (Fig. 2a). The lubricating properties of CS-b-pSBMA at different concentrations were first measured (Fig. 2b). The COF was 0.676 when the concentration of CS-b-pSBMA was 0.01 mg/mL, and it decreased to 0.428 when the concentration of the copolymer increased to 0.1 mg/mL. At concentrations of 1–100 mg/mL, the copolymer exhibited almost super-lubrication effect (COF = 0.013), the reduction of friction coefficient is significantly greater than that of most reported lubricants (Deng, Sun, Ni, & Xiong, 2020; Lei et al., 2022; Liu et al., 2022; Zheng et al., 2019). In contrast, the COF with HA solution at a concentration of 10 mg/mL (a concentration of HA solution commonly used for intra-articular injection in OA treatment (Forsey et al., 2006)) was 0.135, which was consistent with the previous studies (Liu et al., 2020), and approximately one order of magnitude higher than that with the CS-b-pSBMA copolymer at the concentrations of 1–100 mg/mL. In addition, it can be observed that the CS-b-pSBMA lubricant at concentrations of 1–100 mg/mL maintained super-low COF stably over the friction test period of up to 3600 s (equivalent to 1800 friction cycles with the total travelling distance of 36 m) (Fig. 2c), reflecting its long-lasting lubrication performance.

In addition, the lubrication performance of pure CS (1 mg/mL in 1 % acetic acid solution), homopolymer pSBMA (1 mg/mL), and solution of CS and pSBMA mixture (total concentration of 1 mg/mL, containing 0.1 mg/mL of CS and 0.9 mg/mL of pSBMA) was tested. The results showed that the COF values of CS solution, pSBMA solution, and CS + pSBMA solution were 0.346, 0.083, and 0.227, respectively (Fig. 2d), while only CS-b-pSBMA lubricant maintained excellent and stable lubrication performance (Fig. 2e), suggesting that CS, pSBMA, and their mixture failed to achieve comparable lubricating performance as CS-b-pSBMA, and copolymerization of CS and SBMA is significant for improving the lubrication. For CS, due to the limited capability of binding water, its lubricating ability is poor. Generally, pSBMA plays a major lubricating role by binding to large amount water molecules through ion-dipole interaction (Ren et al., 2021). However, owing to the neutral charge of the polymer, pSBMA does not cause electrostatic adsorption at the friction interface, resulting in poor lubrication stability (Li et al., 2022). Consequently, after a simple physical mixing of CS and pSBMA, the lubrication effect would also be limited. In contrast, for CS-b-pSBMA copolymer, the polar amino groups of the CS segment can preferentially adsorb onto the substrate (Wang, Ren, Bai, Liu, & Wu, 2021), which is beneficial to achieve a more stable and excellent lubrication performance under the shear, while the time curve also illustrates this phenomenon (Fig. 2e).

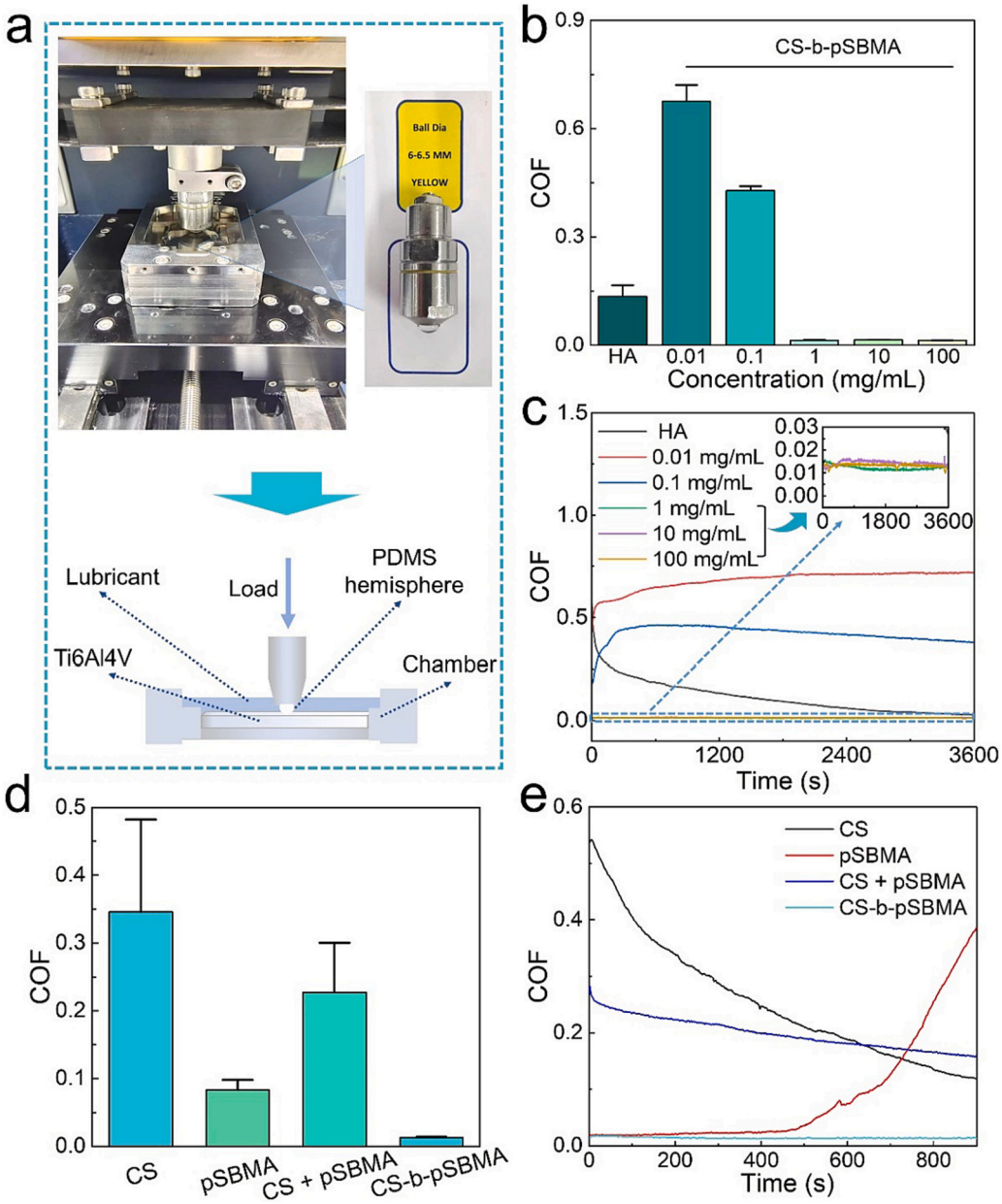

Fig. 2. (a) Photograph and schematic diagram of the setup used in the lubrication test: the friction pair was composed of a PDMS hemisphere and a polished Ti6Al4V alloy plate (the Ti6Al4V alloy plate can be replaced with other materials of the same size). (b) COF values of HA solution (10 mg/mL) and CS-b-pSBMA copolymer solution at different concentrations, and (c) representative COF changes with time in the friction test. (d) COF values, and (e) representative COF-time curves of solutions CS, pSBMA and mixture of CS and pSBMA, CS-b-pSBMA copolymer with the overall concentration of 1 mg/mL in the friction test.

3.3. Applicability of lubricant

The articular cartilage of various joints in the human body is subjected to different pressures, which affect its tribological performance (Morrell, Hodge, Krebs, & Mann, 2005). Herein, the lubricating performance of CS-b-pSBMA copolymer under various magnitudes of loading forces (1, 5, 10, 20, and 50 N, equivalent to pressures of 0.50, 0.86, 1.08, 1.36, and 1.85 MPa, respectively) was investigated (Table S2). The results showed that under the loading pressure tested, the lubricant maintained super-low COF $\leq$ 0.02 (Fig. 3a-b). It should be noted that at a loading force of 1 N, the COF fluctuated in the range of 0.033–0.005 in the test. This is probably because that when the pressure was relatively small, and the PDMS hemisphere connected to the sensor was sensitive to the tiny unevenness of the Ti6Al4V alloy surface, reflecting a fluctuation of the friction during the measurement, in which the average COF kept as low as 0.014. Nevertheless, the CS-b-pSBMA lubricant showed excellent lubrication under a loading force of up to 50 N (upper limit of the tribometer), indicating the copolymer lubricant can maintain good lubrication performance under high loading force in human body.

Furthermore, to investigate the performance of CS-b-pSBMA lubricant in a condition mimicking the articular joint cavity, CS-b-pSBMA copolymer was dissolved in different simulated physiological medium (*i.e.*, 0.9 % NaCl, 10 mM PBS, and 0.1 mg/mL BSA). It can be seen from Fig. 3c that in all the tested medium, the lubricants showed excellent lubrication effect (COF $\leq$ 0.02), and the best lubrication performance was observed in NaCl solution, with a COF as low as 0.008, which showed a super-lubrication effect.

The lubricating effect of CS-b-pSBMA lubricant on smooth glass and common implantable materials such as Al_2O_3 and UHMWPE was also

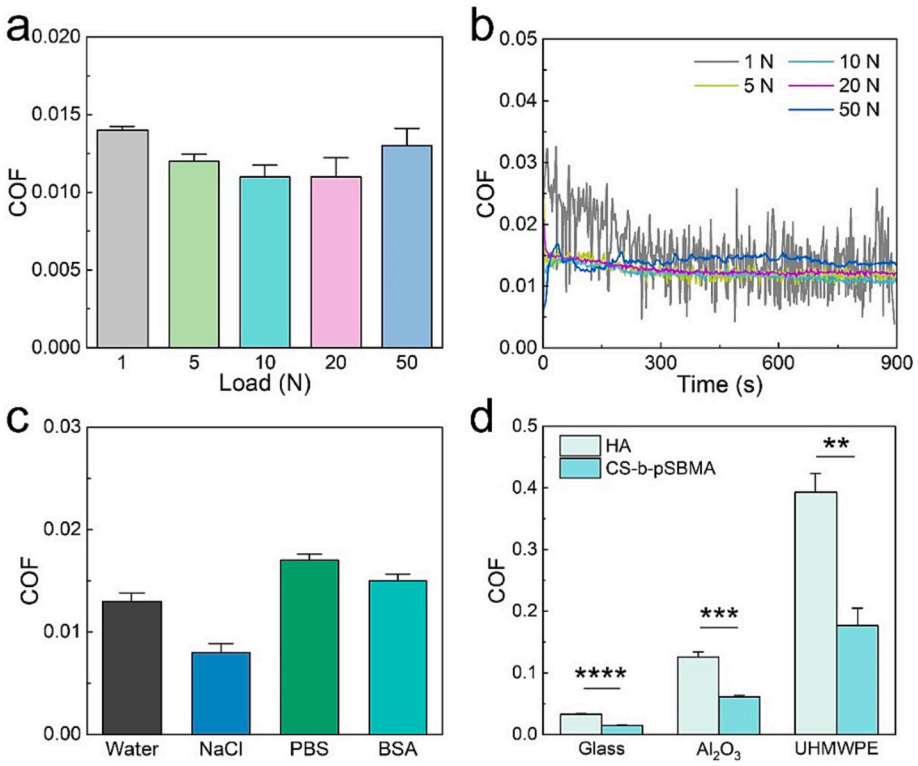

Fig. 3. (a) COF values and (b) representative COF-time curves of CS-b-pSBMA lubricant under different loading forces. (c) COF values of CS-b-pSBMA lubricant in water and different simulated physiological media (0.9 % NaCl, 10 mM PBS, and 0.1 mg/mL BSA). (d) COF values of different substrates (*i.e.*, glass, Al_2O_3 and UHMWPE) with HA or CS-b-pSBMA solution. **/***/**** indicated $p < 0.01/p < 0.001/p < 0.0001$.

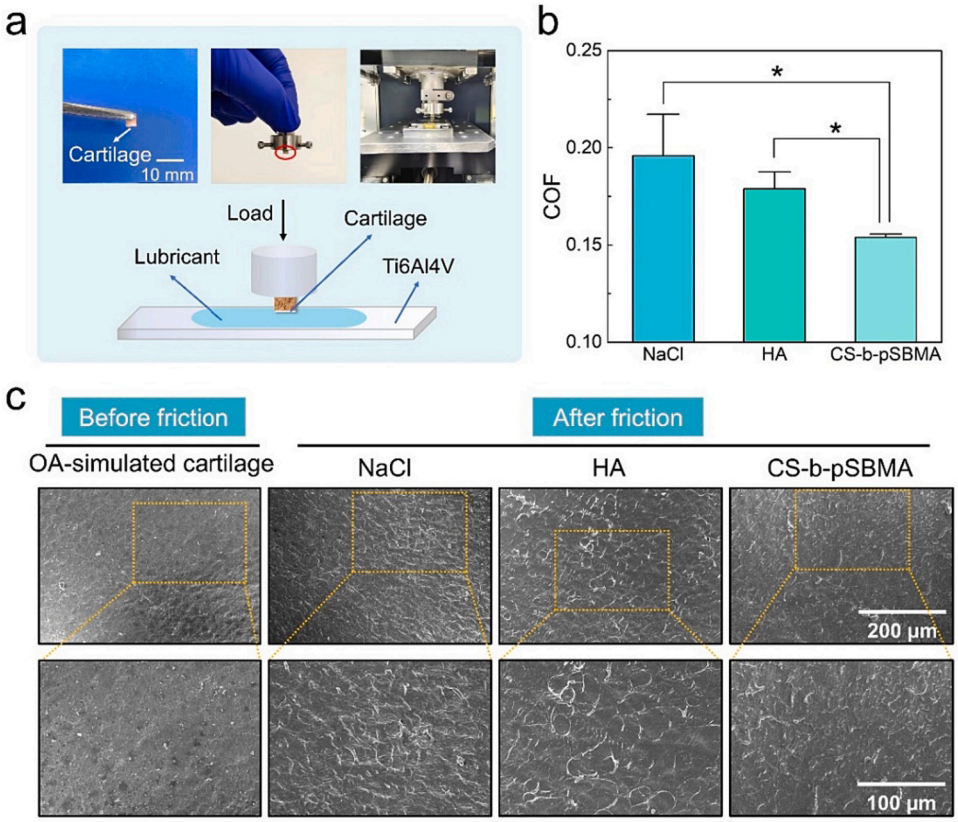

Fig. 4. (a) Photograph and schematic diagram of the setup used in the cartilage lubrication test (cartilage-Ti6Al4V plate pair). A cylindrical bone-cartilage structure with a 4 mm diameter was drilled from a pig femoral head. (b) COF values of different solutions on Ti6Al4V surface. * indicated $p < 0.05$. (c) SEM images of the cartilage pre- and post-friction using different solutions as lubricant.

assessed to explore the potential of the lubricant for artificial joint applications (Fig. 3d). As can be seen, the COF values of glass, Al_2O_3 and UHMWPE were 0.033, 0.126, and 0.393 with HA solution lubricant, and they significantly decreased to 0.015, 0.061, and 0.177, respectively, when CS-b-pSBMA was used as the lubricant, indicating the potential of CS-b-pSBMA as a universal and excellent biomedical lubricant.

3.4. In vitro lubrication on cartilage surface

We further tested the lubricating performance of CS-b-pSBMA copolymer on the surface of digested porcine articular cartilage and compared it with 0.9 % NaCl solution and HA (Fig. 4a-b). CS-b-pSBMA lubricant showed the best cartilage lubrication effect with a COF value of 0.154, compared to that of 0.196 and 0.179 with 0.9 % NaCl solution and HA as the lubricant, respectively. The above results demonstrated that CS-b-pSBMA lubricant could be an option for OA cartilage lubrication treatment.

It is reported that the COF and wear resistance are not directly related, and a low friction COF does not fully represent a good lubricant (Lee et al., 2014). Therefore, the degree of wear of the cartilage surface before and after friction was observed using SEM (Fig. 4c). It can be observed that the texture of the digested cartilage was porous before friction. After friction, due to the reciprocating shear forces and porous surface of cartilage, there were obvious traces of stick-slip with wear (Lee, Banquy, & Israelachvili, 2013). The cartilage surface in the NaCl group was the roughest and showed severe wear marks, whereas the HA and CS-b-pSBMA groups showed mild wear marks. Interestingly, the HA group has a smooth cartilage texture but also pronounced abrasions and wrinkles, which may be related to the fact that HA is a cartilage matrix component with viscoelastic properties. On the one hand, HA can mechanically fill and repair the loose cartilage collagen network. On the other hand, in the case of boundary lubrication, high viscosity HA molecules may easily be extruded out of the friction interface, resulting in increased direct contact and wear between the friction interface (Bonnevie, Galesso, Secchieri, & Bonassar, 2018). While CS-b-pSBMA may be able to persist at the friction interface due to the electrostatic interaction, the formation of a molecular brush layer could reduce the direct contact between the interface, providing good lubrication and reducing the wear of the cartilage.

3.5. Adsorption effect of copolymer on cartilage surface

To investigate the lubrication mechanism, CS-b-pSBMA copolymer was labeled with FITC (Fig. 5a). A cartilage sample was immersed in a FITC-labeled CS-b-pSBMA lubricant solution with a pH of 6 or 13 (to regulate the protonation of amino groups), washed with ultra-pure water to remove the unbonded copolymers, and then the distribution of fluorescent lubricant on the cartilage surface was immediately

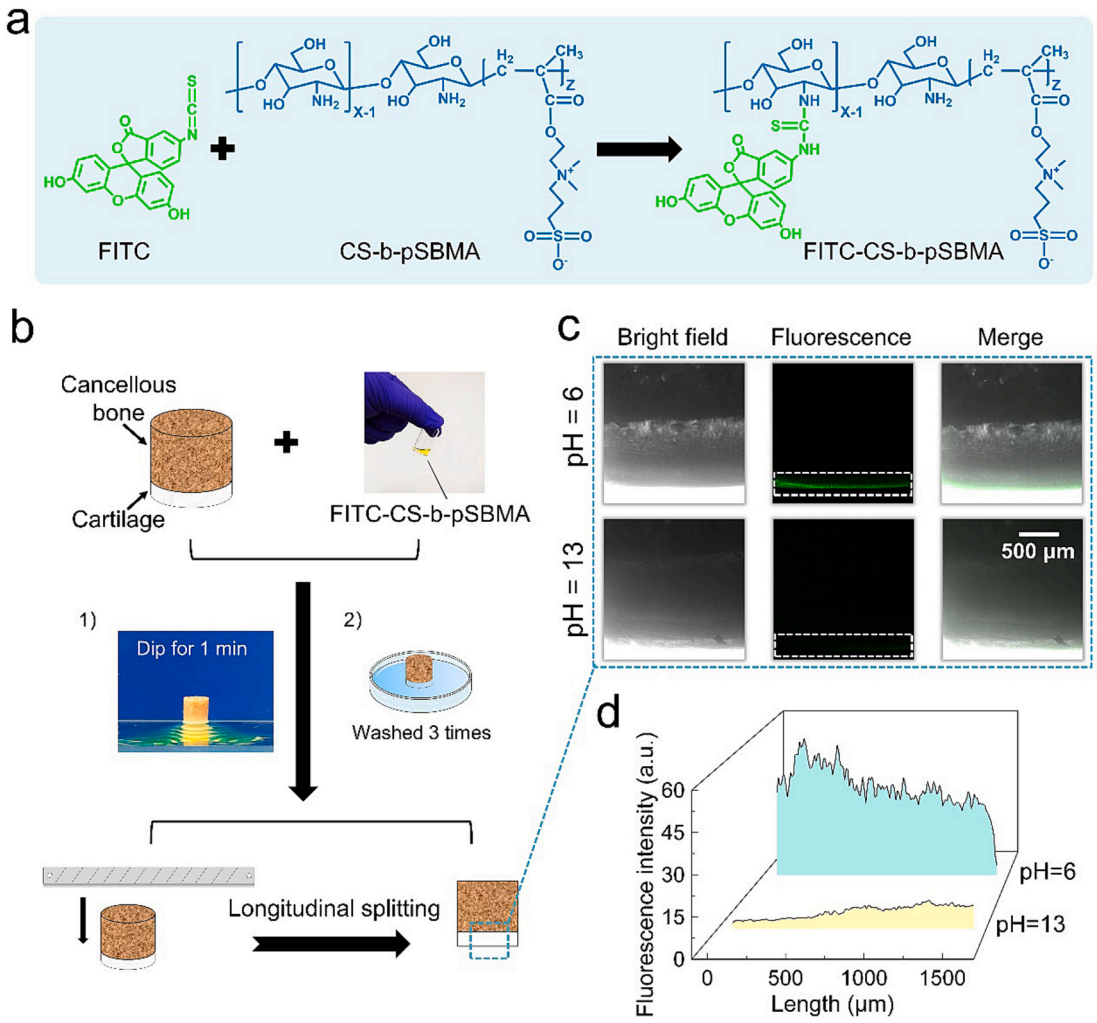

Fig. 5. (a) Schematic illustration of preparation of FITC-labeled CS-b-pSBMA copolymer. (b) Schematic illustration of the experimental procedure for the investigation of FITC-CS-b-pSBMA adsorbing on porcine cartilage. (c) Fluorescence distribution of FITC-labeled CS-b-pSBMA on porcine cartilage. (d) Plot of fluorescence intensity of FITC-labeled CS-b-pSBMA after adsorbing on porcine cartilage.

recorded (Fig. 5b). The results showed that when the pH of the FITC-labeled CS-b-pSBMA solution was 6, the cartilage surface exhibited obvious fluorescence distribution after labelling (Fig. 5c), indicating that the FITC-labeled CS-b-pSBMA copolymers can effectively be adsorbed to the cartilage surface. However, when the solution pH increased to 13, the fluorescence intensity on the cartilage surface decreased, mostly likely because the alkaline condition inhibited the protonation process of the amino group on the CS segment, reducing the electrostatic adsorption of the copolymers to the articular cartilage. The quantitative results also confirmed a higher fluorescence intensity on the cartilage surface at pH 6 than that at pH 13 (Fig. 5d). Therefore, the adsorption mechanism of the lubricant has been proved, which is of great significance for the stable and durable lubrication from the perspective of lubricant molecules adsorbed to the cartilage surface (Scheme 1b).

3.6. *In vitro antibacterial property and biocompatibility*

Intra-articular lubrication is a standard treatment for OA, but the procedure carries a potential risk of infection (Yang, Zhao, et al., 2023). For example, intra-articular injection of HA is often associated with the risk of bacterial infection, which greatly affects the safety and application of intra-articular injection materials (Liu, Shuai, Lu, Yang, & Hu, 2022). Therefore, lubricants with antibacterial properties are also of considerable positive significance in the treatment of OA. Considering CS has bactericidal ability and pSBMA can inhibit the adhesion of bacteria, the CS-b-pSBMA lubricant presents an added advantage in reducing the infection risk during OA treatment. The antibacterial activity of CS-b-pSBMA lubricant against common pathogens *E. coli* and *S. aureus* was investigated. To simulate the favorable environment of synovial fluid (containing proteins, polysaccharides, and so on) to the bacteria, culture medium was added to PBS buffer at a concentration of 1 vol% to create an environment conducive to the growth of bacteria. The results showed that the CS-b-pSBMA lubricant had some antibacterial properties (Fig. 6a-c) and reduced the number of viable *E. coli* by ~1.3 orders of magnitude and that of *S. aureus* by ~1.8 orders of magnitude, after 24 h of incubation, suggesting that CS-b-pSBMA lubricant has the potential to reduce the risk of infection after intra-

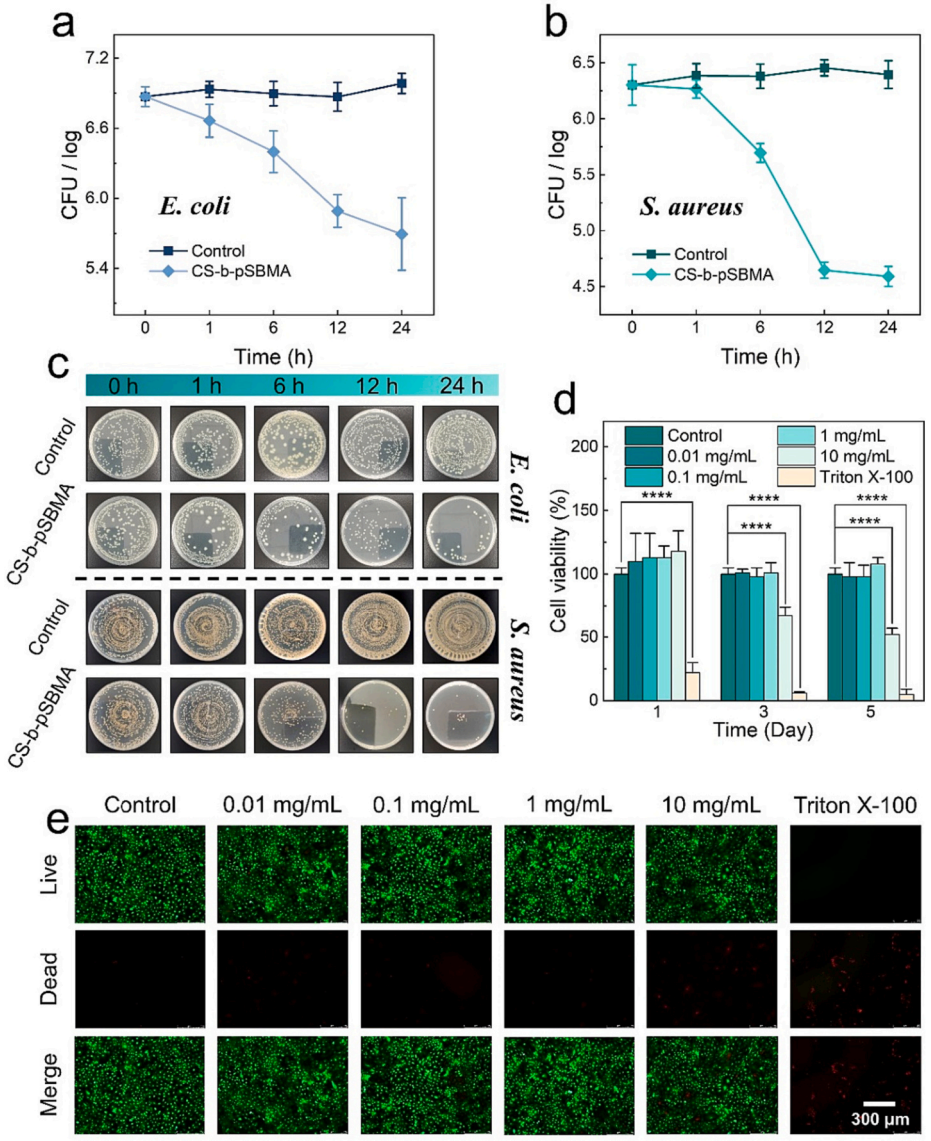

Fig. 6. Bacterial viability of (a) *E. coli* and (b) *S. aureus* after incubation with CS-b-pSBMA copolymer (1 mg/mL) for different periods of time. (c) Representative photographs of bacterial colonies after incubation with CS-b-pSBMA copolymer for different periods of time. (d) Cell viability of rat articular chondrocytes incubated with medium containing different concentrations of CS-b-pSBMA copolymer for different periods. **** indicated $p < 0.0001$. (e) Fluorescence images of chondrocytes after incubation for 3 days and stained with the Live/Dead staining kits.

articular injection.

More importantly, as an injectable lubricant, biocompatibility is the primary prerequisite for its application. Chondrocytes isolated from SD rats knee cartilage were used for the cytotoxicity evaluation of the CS-b-pSBMA lubricant, and the cell viability was assessed using CCK-8 assays and Live/Dead staining (Fig. 6d-e). As can be seen, the CS-b-pSBMA copolymer showed minimal cytotoxicity to the chondrocytes at low concentrations (0.01–1 mg/mL) over 5 days, but did have some inhibitory effect at a high concentration (10 mg/mL) after 3 days (Fig. 6d). Likely, the result of Live/Dead staining showed a similar tendency that a high concentration of CS-b-pSBMA lubricant would inhibit the growth of cells (Fig. 6e). This is probably due to the electronegativity of the cell membrane, while the positively charged CS-b-pSBMA molecules may bind to the cell surface through electrostatic interaction, impeding the material exchange process between cells and medium and inhibiting cell growth. Nevertheless, as the concentration of CS-b-pSBMA lubricant for effective lubrication is not >1 mg/mL, which is in the safe range, it can be considered that the CS-b-pSBMA lubricant has good biocompatibility and could be used for *in vivo* applications.

3.7. Biodegradation of lubricant

It should be noted that one of the major problems with joint injection is that the macromolecular substances injected are easily degraded by the existing enzymes in the body, thus losing their activity or function (Bowman, Awad, Hamrick, Hunter, & Fulzele, 2018). In this study, the lubricating performance of the CS-b-pSBMA copolymer after incubation with LZ and HAase was investigated. HA solution (10 mg/mL) treated with HAase was used as the control. As can be seen, the CS-b-pSBMA lubricant maintained excellent lubrication effects after the treatment of LZ and HAase (Fig. 7a), showing reliable stability. On the contrary, the lubricity of HA after HAase treatment decreased significantly, due to degradation of the HA molecules and decline of solution viscoelasticity, which highlighted the limitation of the unstable lubricity of HA therapy used in clinic practice (Makvandi et al., 2022). The stability of the CS-b-pSBMA lubricant was further evaluated by incubation in a shaking bath at 37 °C for up to 28 days. It was observed that the COF value of CS-b-pSBMA lubricant gradually increased with the increase in incubation time, from 0.013 on Day 1 to 0.018 on Day 7 (Fig. 7b), indicating that the structure of the copolymer may decompose over the prolonged incubation. Nevertheless, the COF of the aged copolymer remained below 0.04 even after 28 days, which could still be considered a good lubricant, better than the original lubricating performance of HA (COF = 0.135), highlighting the potential of the CS-b-pSBMA lubricant to be used for long-term applications.

Rapid biodegradation in the body is a major cause of lubricant failure, leading to frequent injections and limited efficacy, so reliable stability of the lubricants is important (Wan et al., 2022). Furthermore, a fluorescently labeled lubricant (FITC-CS-b-pSBMA) was subcutaneously injected into mice, and the fluorescence signals under the skin of the mice were recorded using IVIS to investigate the retention time of the lubricant *in vivo*. It was observed that the fluorescent signal could remain in the mice subcutaneously for up to 28 days (Fig. 7c), suggesting that CS-b-pSBMA lubricant resisted biodegradation *in vivo* over a long period of time, thus reducing the frequency of lubricant injection in OA therapy.

3.8. In vivo performance

Finally, the therapeutic effect of CS-b-pSBMA lubricant *in vivo* was studied *via* the MIA-induced OA mouse. The timing of animal experiments and processing procedure are shown in Fig. 8a. After two injections, all the mice were executed with the RH knee joint scanned by micro-CT. The micro-CT images after 3D reconstruction showed that the subchondral bone of all the groups except the sham group had been damaged by MIA, while the injury in the NaCl group was more severe than the HA groups and the CS-b-pSBMA lubricant group (Fig. 8b), which had less subchondral bone damage and better integrity after

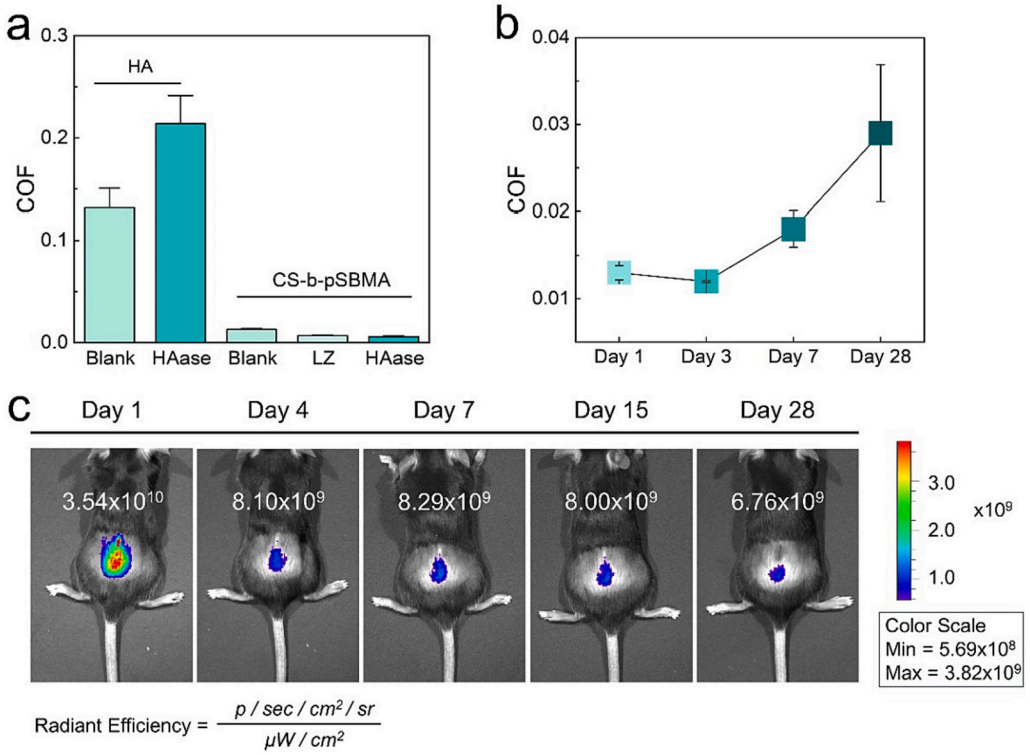

Fig. 7. (a) COF values of CS-b-pSBMA copolymer and HA after LZ and HAase treatment for 48 h (PDMS-Ti6Al4V plate pair). (b) COF values of CS-b-pSBMA lubricant after incubation at 37 °C over 28 days (PDMS-Ti6Al4V plate pair). (c) IVIS images of mice subcutaneously injected with FITC-labeled CS-b-pSBMA solution (1 mg/mL) over 28 days. Numbers in the images show the radiant efficiency of the fluorescence signals on the mouse.

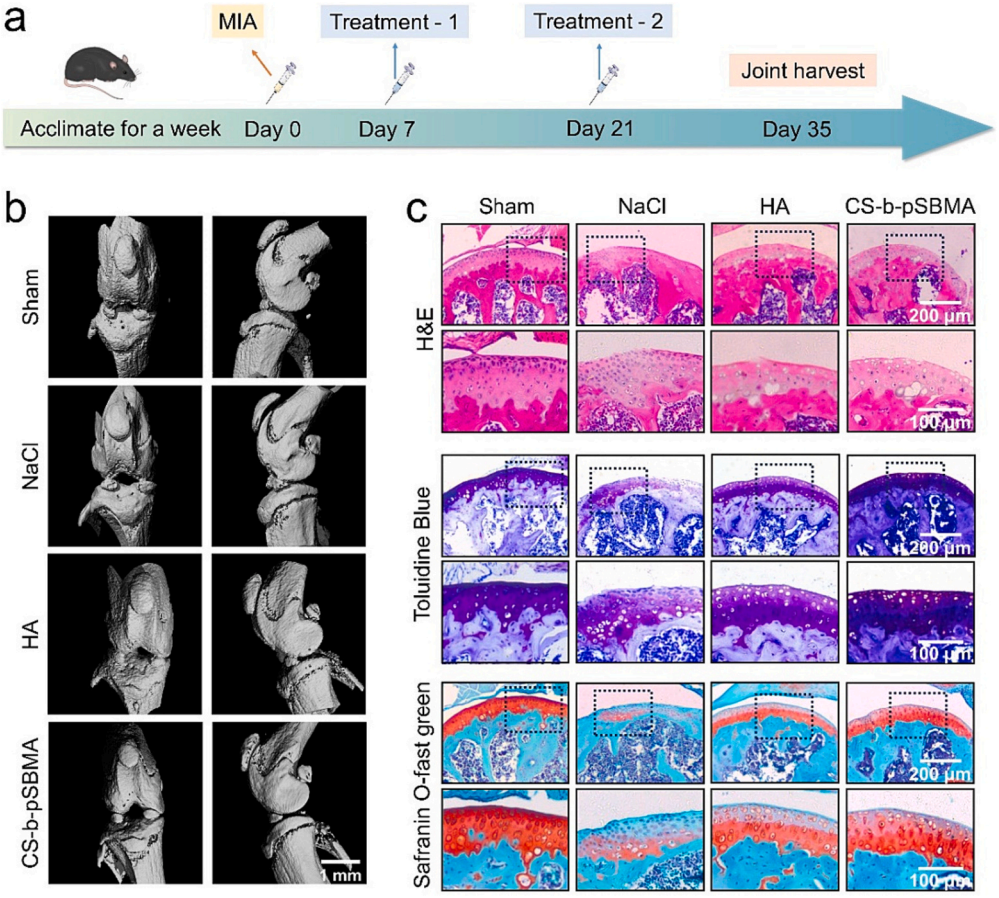

Fig. 8. (a) Schematic timeline of the animal experiment. (b) Representative micro-CT images of the RH knee joint of the mice on Day 35. (c) Representative images of H&E, Toluidine blue and Safranin O-fast green staining of the RH knee joint of mice on Day 35. (For interpretation of the references to colour in this figure legend, the reader is referred to the web version of this article.)

treatment. Histological analysis on articular cartilage was conducted by H&E, toluidine blue, and Safranin O-fast green staining. As illustrated in Fig. 8c, the sham group has a smooth and continuous cartilage surface with clear structure and normal cellularity. The NaCl group revealed cartilage erosion, disorganized structure, apparent cellular abnormalities, and weak staining. In contrast, these degenerative changes were significantly ameliorated in the HA and CS-b-pSBMA groups, while the articular cartilage in the CS-b-pSBMA group has a better structure and smoother surface and a more apparent staining than that in the HA group, indicating that CS-b-pSBMA lubricant could better maintain the articular cartilage composition and relieve symptoms of OA.

Furthermore, SOX9 and MMP13 protein expressions on the cartilages were analyzed by immunohistochemistry. The sham and CS-b-pSBMA groups have significantly higher SOX9 expression protein levels and lowered MMP13 expression protein levels than the NaCl group (Fig. 9). In addition, the level of SOX9 protein expression in the HA group was significantly lower than that in the CS-b-pSBMA group, although it remained higher than that in the NaCl group. This difference could be attributed to the rapid clearance of the HA, which remains in the joint cavity for only 12–24 h (Ma et al., 2022), resulting in limited beneficial effects. In sum, these results demonstrated that the CS-b-pSBMA lubricant can attenuate the progression of OA by reducing cartilage wear and inhibiting cartilage degradation through the lower injection frequency and better lubrication compared to HA.

4. Conclusions

In this study, a biomimetic CS-b-pSBMA lubricant was developed *via* block copolymerization of cheap and readily available CS and SBMA without using toxic organic solvent. The adsorption mechanism of the lubricant was proved for the stable lubrication of the copolymer. Notably, CS-b-pSBMA copolymer showed excellent and superior lubricating effects compared to commonly used HA solution on artificial joint materials including Ti6Al4V alloy, glass, Al_2O_3, and UHMWPE, even digested porcine articular cartilage. In addition, the CS-b-pSBMA lubricant was resistant to enzymatic treatment and had good stability *in vitro* and *in vivo* for up to 4 weeks. *In vitro* tests showed the copolymer had obvious antibacterial properties and good biocompatibility. A preliminary animal study indicated that the CS-b-pSBMA lubricant was able to alleviate the progression of cartilage destruction in OA. It could be expected that with CS-b-pSBMA as an injecting lubricant, the interval for OA treatment could be extended compared to the conventional HA injection. To summarize, this CS-b-pSBMA lubricant achieved the synergistic effects of CS and pSBMA to produce a promising biomimetic lubricant for the treatment of OA.

CRediT authorship contribution statement

Junjie Deng: Conceptualization, Data curation, Investigation, Methodology, Writing – original draft. **Rufang Wei:** Data curation, Methodology. **Haofeng Qiu:** Data curation, Methodology. **Xiang Wu:** Methodology. **Yanyu Yang:** Methodology. **Zhimao Huang:** Methodology. **Jiru Miao:** Methodology. **Ashuang Liu:** Methodology. **Haiyang Chai:** Methodology. **Xiao Cen:** Conceptualization, Methodology, Supervision, Writing – review & editing. **Rong Wang:** Conceptualization, Methodology, Supervision, Writing – review & editing.

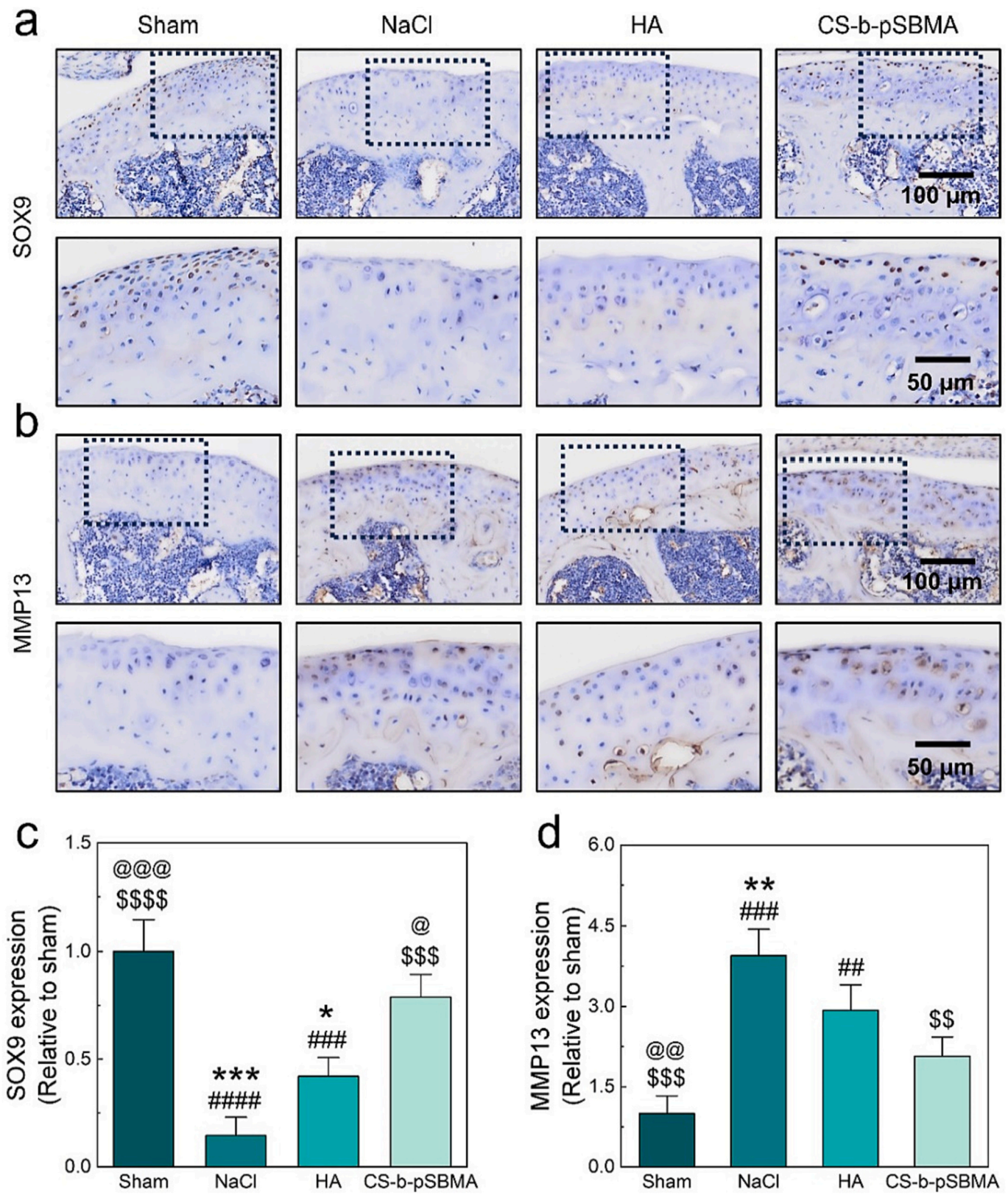

Fig. 9. Immunohistochemistry staining. (a) Representative images of SOX9 protein immunohistochemical staining. (b) Representative images of MMP13 protein immunohistochemical staining. (c) Quantification of relative SOX9 expression. (d) Quantification of relative MMP13 expression. #/##/###/####, $/$$/$$$/$$$$, @/@@/@@@/@@@@ and */**/***/**** indicated $p < 0.05/p < 0.01/p < 0.001/p < 0.0001$ compared to the sham, NaCl, HA and CS-b-pSBMA groups, respectively.

Declaration of competing interest

The authors declare that they have no known competing financial interests or personal relationships that could have appeared to influence the work reported in this paper.

Data availability

Data will be made available on request.

Acknowledgements

This work was funded by the National Key Research and Development Program of China (2018YFE0119400), Youth Innovation Promotion Association CAS (2021296), Key Research and Development Program of Ningbo (2022Z132), Foundation of Director of Ningbo Institute of Materials Technology and Engineering CAS (2021SZKY0301), and Research Funding from West China School/Hospital of Stomatology Sichuan University (RCDWJS2023-17).

Appendix A. Supplementary data

Supplementary data to this article can be found online at https://doi.org/10.1016/j.carbpol.2024.121821.

References

Ahamad, N., Prabhakar, A., Mehta, S., Singh, E., Bhatia, E., Sharma, S., & Banerjee, R. (2020). Trigger-responsive engineered-nanocarriers and image-guided theranostics for rheumatoid arthritis. *Nanoscale, 12*(24), 12673–12697. https://doi.org/10.1039/D0NR01648A

Alfaifi, M. Y., Alkabli, J., & Elshaarawy, R. F. M. (2020). Suppressing of milk-borne pathogenic using new water-soluble chitosan-azidopropanoic acid conjugate: Targeting milk-preservation quality improvement. *International Journal of Biological Macromolecules, 164*, 1519–1526. https://doi.org/10.1016/j.ijbiomac.2020.07.200

Bajpayee, A. G., & Grodzinsky, A. J. (2017). Cartilage-targeting drug delivery: Can electrostatic interactions help? *Nature Reviews Rheumatology, 13*(3), 183–193. https://doi.org/10.1038/nrrheum.2016.210

Bonnevie, E. D., Galesso, D., Secchieri, C., & Bonassar, L. J. (2018). Degradation alters the lubrication of articular cartilage by high viscosity, hyaluronic acid-based lubricants. *Journal of Orthopaedic Research, 36*(5), 1456–1464. https://doi.org/10.1002/jor.23782

Bowman, S., Awad, M. E., Hamrick, M. W., Hunter, M., & Fulzele, S. (2018). Recent advances in hyaluronic acid based therapy for osteoarthritis. *Clinical and Translational Medicine, 7*(1), 6. https://doi.org/10.1186/s40169-017-0180-3

Chang, S.-H., Lin, H.-T. V., Wu, G.-J., & Tsai, G. J. (2015). pH effects on solubility, zeta potential, and correlation between antibacterial activity and molecular weight of chitosan. *Carbohydrate Polymers, 134*, 74–81. https://doi.org/10.1016/j.carbpol.2015.07.072

Chen, H., Sun, T., Yan, Y., Ji, X., Sun, Y., Zhao, X., Qi, J., Cui, W., Deng, L., & Zhang, H. (2020). Cartilage matrix-inspired biomimetic superlubricated nanospheres for treatment of osteoarthritis. *Biomaterials, 242*, Article 119931. https://doi.org/10.1016/j.biomaterials.2020.119931

Chou, Y.-N., Chang, Y., & Wen, T.-C. (2015). Applying Thermosettable Zwitterionic copolymers as general fouling-resistant and thermal-tolerant biomaterial interfaces. *ACS Applied Materials & Interfaces, 7*(19), 10096–10107. https://doi.org/10.1021/acsami.5b01756

Deng, Y., Sun, J., Ni, X., & Xiong, D. (2020). Multilayers of poly(ethyleneimine)/poly (acrylic acid) coatings on Ti6Al4V acting as lubricated polymer-bearing interface. *Journal of Biomedical Materials Research Part B: Applied Biomaterials, 108*(5), 2141–2152. https://doi.org/10.1002/jbm.b.34553

Fang, Z., Li, X., Lei, S., Feng, S., Zhou, C., Tong, X., & Han, R. (2023). Protective effects of Pudilan tablets against osteoarthritis in mice induced by monosodium iodoacetate. *Scientific Reports, 13*(1), Article 1. https://doi.org/10.1038/s41598-023-29976-0

Forsey, R. W., Fisher, J., Thompson, J., Stone, M. H., Bell, C., & Ingham, E. (2006). The effect of hyaluronic acid and phospholipid based lubricants on friction within a human cartilage damage model. *Biomaterials, 27*(26), 4581–4590. https://doi.org/10.1016/j.biomaterials.2006.04.018

Ganji, F., & Abdekhodaie, M. J. (2008). Synthesis and characterization of a new thermosensitive chitosan–PEG diblock copolymer. *Carbohydrate Polymers, 74*(3), 435–441. https://doi.org/10.1016/j.carbpol.2008.03.017

Goto, Y., Masuda, A., & Aiba, T. (2015). In vivo application of chitosan to improve bioavailability of cyanocobalamin, a form of vitamin B12, following intraintestinal administration in rats. *International Journal of Pharmaceutics, 483*(1), 250–255. https://doi.org/10.1016/j.ijpharm.2015.02.016

Hamedi, H., Moradi, S., Hudson, S. M., Tonelli, A. E., & King, M. W. (2022). Chitosan based bioadhesives for biomedical applications: A review. *Carbohydrate Polymers, 282*, Article 119100. https://doi.org/10.1016/j.carbpol.2022.119100

Hamodin, A. G., Elgammal, W. E., Eid, A. M., & Ibrahim, A. G. (2023). Synthesis, characterization, and biological evaluation of new chitosan derivative bearing diphenyl pyrazole moiety. *International Journal of Biological Macromolecules, 243*, Article 125180. https://doi.org/10.1016/j.ijbiomac.2023.125180

Ibrahim, A. G., Fouda, A., Elgammal, W. E., Eid, A. M., Elsenety, M. M., Mohamed, A. E., & Hassan, S. M. (2022). New thiadiazole modified chitosan derivative to control the growth of human pathogenic microbes and cancer cell lines. *Scientific Reports, 12(1), Article 1*. https://doi.org/10.1038/s41598-022-25772-4

Jahn, S., Seror, J., & Klein, J. (2016). Lubrication of articular cartilage. *Annual Review of Biomedical Engineering, 18*(1), 235–258. https://doi.org/10.1146/annurev-bioeng-081514-123305

Jin, T., Wu, D., Liu, X.-M., Xu, J.-T., Ma, B.-J., Ji, Y., Jin, Y.-Y., Wu, S.-Y., Wu, T., & Ma, K. (2020). Intra-articular delivery of celastrol by hollow mesoporous silica nanoparticles for pH-sensitive anti-inflammatory therapy against knee osteoarthritis. *Journal of Nanobiotechnology, 18*(1), 94. https://doi.org/10.1186/s12951-020-00651-0

Kamal, I., Khedr, A. I. M., Alfaifi, M. Y., Elbehairi, S. E. I., Elshaarawy, R. F. M., & Saad, A. S. (2021). Chemotherapeutic and chemopreventive potentials of ρ-coumaric acid – Squid chitosan nanogel loaded with Syzygium aromaticum essential oil. *International Journal of Biological Macromolecules, 188*, 523–533. https://doi.org/10.1016/j.ijbiomac.2021.08.038

Kar, A., Ahamad, N., Dewani, M., Awasthi, L., Patil, R., & Banerjee, R. (2022). Wearable and implantable devices for drug delivery: Applications and challenges. *Biomaterials, 283*, Article 121435. https://doi.org/10.1016/j.biomaterials.2022.121435

Lee, D. W., Banquy, X., Das, S., Cadirov, N., Jay, G., & Israelachvili, J. (2014). Effects of molecular weight of grafted hyaluronic acid on wear initiation. *Acta Biomaterialia, 10*(5), 1817–1823. https://doi.org/10.1016/j.actbio.2014.01.013

Lee, D. W., Banquy, X., & Israelachvili, J. N. (2013). Stick-slip friction and wear of articular joints. *Proceedings of the National Academy of Sciences, 110*(7), E567–E574. https://doi.org/10.1073/pnas.1222470110

Lee, D. W., Lim, C., Israelachvili, J. N., & Hwang, D. S. (2013). Strong adhesion and cohesion of chitosan in aqueous solutions. *Langmuir, 29*(46), 14222–14229. https://doi.org/10.1021/la403124u

Lei, Y., Wang, X., Liao, J., Shen, J., Li, Y., Cai, Z., Hu, N., Luo, X., Cui, W., & Huang, W. (2022). Shear-responsive boundary-lubricated hydrogels attenuate osteoarthritis. *Bioactive Materials, 16*, 472–484. https://doi.org/10.1016/j.bioactmat.2022.02.016

Li, J., Sun, C., Tao, W., Cao, Z., Qian, H., Yang, X., & Wang, J. (2018). Photoinduced PEG deshielding from ROS-sensitive linkage-bridged block copolymer-based nanocarriers for on-demand drug delivery. *Biomaterials, 170*, 147–155. https://doi.org/10.1016/j.biomaterials.2018.04.015

Li, L., Yan, B., Zhang, L., Tian, Y., & Zeng, H. (2015). Mussel-inspired antifouling coatings bearing polymer loops. *Chemical Communications, 51*(87), 15780–15783. https://doi.org/10.1039/C5CC06852E

Li, Q., Wen, C., Yang, J., Zhou, X., Zhu, Y., Zheng, J., … Zhang, P. (2022). Zwitterionic biomaterials. *Chemical Reviews, 122*(23), 17073–17154. https://doi.org/10.1021/acs.chemrev.2c00344

Lim, C., Hwang, D. S., & Lee, D. W. (2021). Intermolecular interactions of chitosan: Degree of acetylation and molecular weight. *Carbohydrate Polymers, 259*, Article 117782. https://doi.org/10.1016/j.carbpol.2021.117782

Lim, C., Lee, D. W., Israelachvili, J. N., Jho, Y., & Hwang, D. S. (2015). Contact time- and pH-dependent adhesion and cohesion of low molecular weight chitosan coated surfaces. *Carbohydrate Polymers, 117*, 887–894. https://doi.org/10.1016/j.carbpol.2014.10.033

Lin, W., & Klein, J. (2021). Recent Progress in cartilage lubrication. *Advanced Materials, 33*(18), 2005513. https://doi.org/10.1002/adma.202005513

Liu, G., Feng, Y., Zhao, N., Chen, Z., Shi, J., & Zhou, F. (2022). Polymer-based lubricating materials for functional hydration lubrication. *Chemical Engineering Journal, 429*, Article 132324. https://doi.org/10.1016/j.cej.2021.132324

Liu, W., Ma, M., Lei, Z., Xiong, Z., Tao, T., Lei, P., Hu, Y., Jiang, X., & Xiao, J. (2022). Intra-articular injectable hydroxypropyl chitin/hyaluronic acid hydrogel as bio-lubricant to attenuate osteoarthritis progression. *Materials & Design, 217*, Article 110579. https://doi.org/10.1016/j.matdes.2022.110579

Liu, Y., Shuai, C., Lu, G., Yang, X., & Hu, X. (2022). Preparation of polyethylene glycol brush grafted from the surface of nitrile butadiene rubber with excellent tribological performance under aqueous lubrication. *Materials & Design, 224*, Article 111310. https://doi.org/10.1016/j.matdes.2022.111310

Liu, Z., Lin, W., Fan, Y., Kampf, N., Wang, Y., & Klein, J. (2020). Effects of Hyaluronan molecular weight on the lubrication of cartilage-emulating boundary layers. *Biomacromolecules, 21*(10), 4345–4354. https://doi.org/10.1021/acs.biomac.0c01151

Ma, L., Zheng, X., Lin, R., Sun, A. R., Song, J., Ye, Z., … Liu, Y. (2022). Knee osteoarthritis therapy: Recent advances in intra-articular drug delivery systems. *Drug Design, Development and Therapy, 16*, 1311–1347. https://doi.org/10.2147/DDDT.S357386

Macirowski, T., Tepic, S., & Mann, R. W. (1994). Cartilage stresses in the human hip joint. *Journal of Biomechanical Engineering, 116*(1), 10–18. https://doi.org/10.1115/1.2895693

Makvandi, P., Della Sala, F., di Gennaro, M., Solimando, N., Pagliuca, M., & Borzacchiello, A. (2022). A hyaluronic acid-based formulation with simultaneous local drug delivery and antioxidant ability for active Viscosupplementation. *ACS Omega, 7*(12), 10039–10048. https://doi.org/10.1021/acsomega.1c05622

Morrell, K. C., Hodge, W. A., Krebs, D. E., & Mann, R. W. (2005). Corroboration of in vivo cartilage pressures with implications for synovial joint tribology and osteoarthritis causation. *Proceedings of the National Academy of Sciences, 102*(41), 14819–14824. https://doi.org/10.1073/pnas.0507117102

Nasr, A. M., Aboelenin, S. M., Alfaifi, M. Y., Shati, A. A., Elbehairi, S. E. I., Elshaarawy, R. F. M., & Elwahab, N. H. A. (2022). Quaternized chitosan thiol hydrogel-thickened Nanoemulsion: A multifunctional platform for upgrading the topical applications of virgin olive oil. *Pharmaceutics, 14(7), Article 7*. https://doi.org/10.3390/pharmaceutics14071319

Pap, T., & Korb-Pap, A. (2015). Cartilage damage in osteoarthritis and rheumatoid arthritis—Two unequal siblings. *Nature reviews. Rheumatology, 11(10), Article 10*. https://doi.org/10.1038/nrrheum.2015.95

Park, S., Kim, M., Park, J., Choi, W., Hong, J., Lee, D. W., & Kim, B.-S. (2021). Mussel-inspired multiloop Polyethers for antifouling surfaces. *Biomacromolecules, 22*(12), 5173–5184. https://doi.org/10.1021/acs.biomac.1c01124

Qin, L., Sun, H., Hafezi, M., & Zhang, Y. (2019). Polydopamine-assisted immobilization of chitosan brushes on a textured CoCrMo alloy to improve its tribology and biocompatibility. *Materials, 12(18), Article 18*. https://doi.org/10.3390/ma12183014

Ren, K., Ke, X., Chen, Z., Zhao, Y., He, L., Yu, P., Xing, J., Luo, J., Xie, J., & Li, J. (2021). Zwitterionic polymer modified xanthan gum with collagen II-binding capability for lubrication improvement and ROS scavenging. *Carbohydrate Polymers, 274*, Article 118672. https://doi.org/10.1016/j.carbpol.2021.118672

Rong, M., Liu, H., Scaraggi, M., Bai, Y., Bao, L., Ma, S., … Zhou, F. (2020). High lubricity meets load capacity: Cartilage mimicking bilayer structure by brushing up stiff hydrogels from subsurface. *Advanced Functional Materials, 30*(39), 2004062. https://doi.org/10.1002/adfm.202004062

Shin, E., Lim, C., Kang, U. J., Kim, M., Park, J., Kim, D., … Kim, B.-S. (2020). Mussel-inspired Copolyether loop with superior antifouling behavior. *Macromolecules, 53*(9), 3551–3562. https://doi.org/10.1021/acs.macromol.0c00481

Vandeweerd, J.-M., Innocenti, B., Rocasalbas, G., Gautier, S. E., Douette, P., Hermitte, L., … Chausson, M. (2021). Non-clinical assessment of lubrication and free radical scavenging of an innovative non-animal carboxymethyl chitosan biomaterial for viscosupplementation: An in-vitro and ex-vivo study. *PLoS One, 16*(10), Article e0256770. https://doi.org/10.1371/journal.pone.0256770

Wan, H., Ren, K., Kaper, H. J., & Sharma, P. K. (2020). A bioinspired mucoadhesive restores lubrication of degraded cartilage through reestablishment of lamina splendens. *Colloids and Surfaces B: Biointerfaces, 193*, Article 110977. https://doi.org/10.1016/j.colsurfb.2020.110977

Wan, H., Zhao, X., Lin, C., Kaper, H. J., & Sharma, P. K. (2020). Nanostructured coating for biomaterial lubrication through biomacromolecular recruitment. *ACS Applied Materials & Interfaces, 12*(21), 23726–23736. https://doi.org/10.1021/acsami.0c04899

Wan, L., Wang, Y., Tan, X., Sun, Y., Luo, J., & Zhang, H. (2022). Biodegradable lubricating mesoporous silica nanoparticles for osteoarthritis therapy. *Friction, 10*(1), 68–79. https://doi.org/10.1007/s40544-020-0391-2

Wang, R., Neoh, K. G., & Kang, E.-T. (2015). Integration of antifouling and bactericidal moieties for optimizing the efficacy of antibacterial coatings. *Journal of Colloid and Interface Science, 438*, 138–148. https://doi.org/10.1016/j.jcis.2014.09.070

Wang, T., Ren, X., Bai, Y., Liu, L., & Wu, G. (2021). Adhesive and tough hydrogels promoted by quaternary chitosan for strain sensor. *Carbohydrate Polymers, 254*, Article 117298. https://doi.org/10.1016/j.carbpol.2020.117298

Wang, W., Xue, C., & Mao, X. (2020). Chitosan: Structural modification, biological activity and application. *International Journal of Biological Macromolecules, 164*, 4532–4546. https://doi.org/10.1016/j.ijbiomac.2020.09.042

Xie, R., Yao, H., Mao, A. S., Zhu, Y., Qi, D., Jia, Y., … Mao, C. (2021). Biomimetic cartilage-lubricating polymers regenerate cartilage in rats with early osteoarthritis. *Nature. Biomedical Engineering, 5(10), Article 10*. https://doi.org/10.1038/s41551-021-00785-y

Yan, Y., Sun, T., Zhang, H., Ji, X., Sun, Y., Zhao, X., … Zhang, H. (2019). Euryale Ferox seed-inspired Superlubricated nanoparticles for treatment of osteoarthritis. *Advanced Functional Materials, 29*(4), 1807559. https://doi.org/10.1002/adfm.201807559

Yang, L., Huang, H., Zeng, H., Zhao, X., Wang, R., Ma, Z., Fan, Z., Liang, Y., Ma, S., & Zhou, F. (2023). Biomimetic chitosan nanoparticles with simultaneous water lubricant and anti-inflammatory. *Carbohydrate Polymers, 304*, Article 120503. https://doi.org/10.1016/j.carbpol.2022.120503

Yang, L., Zhao, X., Liao, X., Wang, R., Fan, Z., Ma, S., & Zhou, F. (2023). Biomimetic chitosan-derived bifunctional lubricant with superior antibacterial and hydration lubrication performances. *Journal of Colloid and Interface Science, 629*, 859–870. https://doi.org/10.1016/j.jcis.2022.09.098

Yang, Y., Zhu, W., Cheng, L., Cai, R., Yi, X., He, J., Pan, X., Yang, L., Yang, K., Liu, Z., Tan, W., & Chen, M. (2020). Tumor microenvironment (TME)-activatable circular aptamer-PEG as an effective hierarchical-targeting molecular medicine for photodynamic therapy. *Biomaterials, 246*, Article 119971. https://doi.org/10.1016/j.biomaterials.2020.119971

Yuan, H., Mears, L. L. E., Wang, Y., Su, R., Qi, W., He, Z., & Valtiner, M. (2023). Lubricants for osteoarthritis treatment: From natural to bioinspired and alternative strategies. *Advances in Colloid and Interface Science, 311*, Article 102814. https://doi.org/10.1016/j.cis.2022.102814

Yue, Q., Lei, L., Gu, Y., Chen, R., Zhang, M., Yu, H., … Zhou, F. (2022). Bioinspired polysaccharide-derived Zwitterionic brush-like copolymer as an injectable biolubricant for arthritis treatment. *Advanced Healthcare Materials, 11*(13), 2200090. https://doi.org/10.1002/adhm.202200090

Zhang, M., Peng, X., Ding, Y., Ke, X., Ren, K., Xin, Q., Qin, M., Xie, J., & Li, J. (2023). A cyclic brush zwitterionic polymer based pH-responsive nanocarrier-mediated dual drug delivery system with lubrication maintenance for osteoarthritis treatment. *Materials Horizons.*. https://doi.org/10.1039/D3MH00218G

Zheng, Y., Yang, J., Liang, J., Xu, X., Cui, W., Deng, L., & Zhang, H. (2019). Bioinspired hyaluronic acid/Phosphorylcholine polymer with enhanced lubrication and anti-inflammation. *Biomacromolecules, 20*(11), 4135–4142. https://doi.org/10.1021/acs.biomac.9b00964

Zhu, Z., Gao, Q., Long, Z., Huo, Q., Ge, Y., Vianney, N., … Wang, B. (2021). Polydopamine/poly(sulfobetaine methacrylate) co-deposition coatings triggered by CuSO4/H2O2 on implants for improved surface hemocompatibility and antibacterial activity. *Bioactive Materials, 6*(8), 2546–2556. https://doi.org/10.1016/j.bioactmat.2021.01.025